

1           **Impairments in the mechanical effectiveness of reactive balance control**  
2                           **strategies during walking in people post-stroke**

3                           **Chang Liu<sup>1,a</sup>, Jill L. McNitt-Gray<sup>1,2</sup>, and James Finley<sup>1,3,4</sup>**

4           <sup>1</sup>Department of Biomedical Engineering, University of Southern California, Los Angeles, USA

5

6           <sup>2</sup>Department of Biological Science, University of Southern California, Los Angeles, USA

7

8           <sup>3</sup>Division of Biokinesiology and Physical Therapy, University of Southern California, Los  
9 Angeles, USA

10

11           <sup>4</sup>Neuroscience Graduate Program, University of Southern California, Los Angeles, CA, 90089

12

13           <sup>a</sup>Current address: Department of Biomedical Engineering, University of Florida, Gainesville,

14 USA

15

16           \* Correspondence:

17           liu.chang1@ufl.edu

18           jmfinley@usc.edu

19

20           Keywords: balance, stroke, angular impulse, angular momentum, gait, reactive control, forward

21           loss of balance

22

## 23 **Abstract**

24        People post-stroke have an increased risk of falls compared to neurotypical individuals,  
25 partly resulting from an inability to generate appropriate reactions to restore balance. However,  
26 few studies investigated the effect of paretic deficits on the mechanics of reactive control  
27 strategies following forward losses of balance during walking. Here, we characterized the  
28 biomechanical consequences of reactive control strategies following perturbations induced by the  
29 treadmill belt accelerations. Thirty-eight post-stroke participants and thirteen age-matched and  
30 speed-matched neurotypical participants walked on a dual-belt treadmill while receiving  
31 perturbations that induced a forward loss of balance. We computed whole-body angular  
32 momentum and angular impulse using segment kinematics and reaction forces to quantify the  
33 effect of impulse generation by both the leading and trailing limbs in response to perturbations in  
34 the sagittal plane. We found that perturbations to the paretic limb led to larger increases in  
35 forward angular momentum during the perturbation step than perturbations to the non-paretic  
36 limb or to neurotypical individuals. To recover from the forward loss of balance, neurotypical  
37 individuals coordinated reaction forces generated by both legs to decrease the forward angular  
38 impulse relative to the pre-perturbation step. They first decreased the forward pitch angular  
39 impulse during the perturbation step. Then, during the first recovery step, they increased the  
40 backward angular impulse by the leading limb and decreased the forward angular impulse by the  
41 trailing limb. In contrast to neurotypical participants, people post-stroke did not reduce the  
42 forward angular impulse generated by the stance limb during the perturbed step. They also did  
43 not increase leading limb angular impulse or decrease the forward trailing limb angular impulse  
44 using their paretic limb during the first recovery step. Lastly, post-stroke individuals who scored  
45 poorer on clinical assessments of balance and had greater motor impairment made less use of the  
46 paretic limb to reduce forward momentum. Overall, these results suggest that paretic deficits  
47 limit the ability to recover from forward loss of balance. Future perturbation-based balance  
48 training targeting reactive stepping response in stroke populations may benefit from improving  
49 the ability to modulate paretic ground reaction forces to better control whole-body dynamics.

50  
51  
52

## 53 1 Introduction

54 People post-stroke have an increased risk of falls relative to neurotypical individuals  
55 (Weerdesteyn et al., 2008) and this may be due, in part, to impairments in their ability to  
56 generate appropriate reactive strategies following a loss of balance. These impairments result  
57 from a combination of delayed muscle activation to external perturbations (Kirker et al., 2000;  
58 Marigold et al., 2004), abnormal muscle activation patterns (Higginson et al., 2006), and  
59 weakness (Olney & Richards, 1996). In addition, trips or slips, which commonly occur in the  
60 direction of walking, are one of the most prevalent causes of falls among people post-stroke  
61 (Schmid et al., 2013). Although prior studies have examined the dynamics of backward losses of  
62 balance during stance (Patel & Bhatt, 2017; Salot et al., 2016) and walking post-stroke (Dusane  
63 et al., 2021; Kajrolkar et al., 2014; Kajrolkar & Bhatt, 2016), few have investigated the  
64 mechanics and recovery strategies following forward losses of balance during walking.

65 When responding to forward losses of balance during walking, neurotypical individuals  
66 adopt a sequence of reactive control strategies across multiple steps to counteract the forward  
67 rotation of the body (Debelle et al., 2020). For example, when people trip over an obstacle, their  
68 first opportunity to recover balance involves modulating the support limb's push-off force to  
69 reduce forward angular momentum (Pijnappels et al., 2005). Next, people often increase the  
70 length of the recovery step to reduce forward momentum while walking (Debelle et al., 2020;  
71 Golyski et al., 2022; Mathiyakom & McNitt-Gray, 2008; Roeles et al., 2018; Vlutters et al.,  
72 2016). As a result, the ground reaction forces of the leading recovery limb and the perturbed  
73 trailing limb combine to generate a backward moment about the center of mass (CoM) and help  
74 arrest the forward rotation of the body (Mathiyakom & McNitt-Gray, 2008).

75           However, sensorimotor deficits in people post-stroke may prevent them from executing  
76 successful reactions to forward losses of balance while walking. If a perturbation occurs during  
77 paretic stance, the paretic leg may be too weak to adequately support the body or it may lack the  
78 dexterity to properly regulate the body's momentum (Arene & Hidler, 2009; Honda et al., 2019;  
79 Nott et al., 2014; Roerdink et al., 2009). Therefore, people post-stroke may not have sufficient  
80 time to step further forward with the non-paretic limb and arrest forward momentum.  
81 Conversely, if a perturbation occurs during non-paretic stance, they may have difficulty initiating  
82 a successful stepping response with the paretic leg to help restore balance due to deficits in  
83 paretic propulsion (Allen et al., 2014; Chen et al., 2005; Lauzière et al., 2015) and hip flexion  
84 (Rybar et al., 2014). However, it has yet to be determined how paretic deficits impact the  
85 biomechanical consequences of reactive response to forward losses of balance or whether these  
86 effects differ following perturbations to the paretic versus non-paretic limbs.

87           Here, our objective was to determine how stroke influences the biomechanical  
88 consequences of reactive control strategies following sudden treadmill accelerations (Figure 1).  
89 To counteract the increase in forward angular momentum following a perturbation, participants  
90 could use a combination of recovery strategies during the perturbation and recovery steps. First,  
91 they could reduce the forward angular impulse during the single stance phase following the  
92 perturbation. Second, they could increase the backward angular impulse generated by the leading  
93 limb during the recovery step. Finally, they could also decrease the forward angular impulse  
94 generated by the trailing limb during the first recovery step. We hypothesized that treadmill  
95 accelerations would cause larger increases in forward angular momentum in people post-stroke  
96 compared to neurotypical control individuals regardless of the side of the perturbation as post-  
97 stroke deficits may prevent these individuals from generating adequate reactive control

98 strategies. We also expected that perturbations of the paretic leg would lead to greater increases  
99 in forward angular momentum than perturbations of the non-paretic side due to deficits in the  
100 ability of the paretic leg to support body weight (Figure 1A). When considering the  
101 biomechanical consequences of the reactive responses, we hypothesized that neurotypical  
102 participants would have larger contributions to the reduction of forward angular momentum from  
103 both the perturbed limb and the recovery limb compared with those of people post-stroke (Figure  
104 1B-C). Lastly, we hypothesized that post-stroke participants would generate smaller reductions  
105 in forward angular impulse by the perturbed limb and larger increases in backward angular  
106 impulse using the recovery limb during the first recovery step following paretic versus non-  
107 paretic perturbations (Figure 1B-C).

## 108 **2 Methods**

### 109 **2.1 Participants**

110 We recruited 38 people post-stroke (Table 1) from the IRB-approved, USC Registry for  
111 Aging and Rehabilitation, the USC Physical Therapy Associates Clinic, and Rancho Los Amigos  
112 National Rehabilitation Center. Inclusion criteria for the stroke survivors were the following: 1) a  
113 unilateral brain lesion 2) paresis confined to one side, 3) ability to walk on the treadmill for five  
114 minutes without holding on to any support. Use of ankle-foot orthoses was permitted during the  
115 experiment. We also recruited 13 age-matched neurotypical participants from the community.  
116 Exclusion criteria for neurotypical participants were neurological, cardiovascular, orthopedic,  
117 and psychiatric diagnoses. Study procedures were approved by the Institutional Review Board at  
118 the University of Southern California and all participants provided written, informed consent

119 before testing began. All aspects of the study conformed to the principles described in the  
120 Declaration of Helsinki.

## 121 **2.2 Experimental protocol**

122 The experimental protocol for post-stroke participants has been described previously  
123 (Buurke et al., 2020), and we provide a summary of the procedures and setup below. The  
124 complete protocol consisted of a set of clinical assessments and walking trials on the treadmill.  
125 Before the walking trials, we evaluated motor impairment using the lower extremity portion of  
126 the Fugl-Meyer Assessment (FM) (Fugl-Meyer et al., 1975), static balance using Berg Balance  
127 Scale (BBS)(Berg et al., 1992), static and dynamic balance during locomotion using the  
128 Functional Gait Assessment (FGA)(Leddy et al., 2011), and over-ground walking speed using  
129 the 10-meter walking test. Participants also completed questionnaires about balance confidence  
130 using the Activity-Specific Balance Confidence Scale (ABC) (Powell & Myers, 1995). Higher  
131 scores on all these assessments indicated better balance control or higher balance confidence.  
132 Lastly, we completed a Fall History Questionnaire for participants who experienced at least one  
133 fall within the past year. After clinical evaluations, we instructed stroke participants to walk on  
134 the dual-belt treadmill (Bertec, Columbus, OH, USA). A harness was provided to prevent the  
135 participants from falling but no body weight support was provided. First, the participants walked  
136 on the treadmill to familiarize themselves with the experimental setup. To identify participants'  
137 preferred walking speed on the treadmill, we started from 70% of the speed obtained from a 10-  
138 meter walking test and adjusted their walking speed by 0.05 m/s increments or decrements until  
139 the participants verbally indicated that they achieved their preferred walking speed (Park et al.,  
140 2021). Participants then walked for three minutes at their self-selected speed. After the  
141 unperturbed walking trial, participants completed a familiarization trial with at least two sudden

142 treadmill accelerations which were triggered at foot-strike based on the ground reaction forces  
143 recorded by the treadmill's force plates. Finally, participants completed two trials of three  
144 minutes at their self-selected speed during which they received six accelerations to the treadmill  
145 belts on each side.

146 Neurotypical participants also completed a set of clinical assessments including the ABC,  
147 FES, BBS, and 10-meter walking test. We instructed the participants to walk at matched speeds  
148 with a stroke participant of similar age, and they completed one unperturbed walking trial and  
149 one perturbed trial at this speed. For the perturbed trial, 10 perturbations occurred on each side.

150 For both groups, treadmill accelerations were triggered at random intervals within 15 to  
151 25 steps after the previous perturbation to allow participants to reestablish their walking patterns.  
152 Each perturbation was characterized by a trapezoidal speed profile in which the speed increased  
153 by 0.2 m/s at an acceleration of  $3 \text{ m/s}^2$ , was held for 0.7 s, and then decelerated back to the self-  
154 selected speed during the swing phase of the perturbed leg. Between each trial, stroke  
155 participants had breaks of at least three minutes to minimize fatigue while control participants  
156 were given breaks as needed. Participants did not hold on to handrails while walking on the  
157 treadmill.

### 158 **2.3 Data Acquisition**

159 A ten-camera motion capture system (Qualisys AB, Gothenburg, Sweden) recorded 3D  
160 marker kinematics at 100 Hz and ground reaction forces at 1000 Hz. We placed a set of 14 mm  
161 spherical markers on anatomical landmarks (Havens et al., 2018; Song et al., 2012) and placed  
162 marker clusters on the upper arms, forearms, thighs, shanks, and the back of heels. Marker  
163 positions were calibrated during a five-second standing trial at the beginning of each trial. We  
164 removed all joint markers after the calibration.

## 165 **2.4 Data Processing**

166 We post-processed the kinematic and kinetic data in Visual3D (C-Motion, Rockville,  
167 MD, USA) and Matlab 2020b (Mathworks, USA) to compute variables of interest. Marker  
168 positions and ground reaction forces were low-pass filtered by 4<sup>th</sup> order Butterworth filters with  
169 cutoff frequencies of 6 Hz and 20 Hz, respectively based on previous literature (Kurz et al.,  
170 2012; Reisman et al., 2009; Winter, 2009). We defined foot strike as the point when the vertical  
171 ground reaction force became greater than 150N and foot off as the point when vertical ground  
172 reaction force became less than 150N (Liu et al., 2018). We removed the perturbations that  
173 occurred more than ~150 ms after foot strike. We included a median of 11 (interquartile range:  
174 3.5) perturbations per side for each stroke participant and a median of 10 (interquartile range:  
175 0.5) perturbations per side for each age-matched control participant. We categorized the pre-  
176 perturbation steps as the last two steps before the perturbation occurred (Pre-PTB<sub>1-2</sub>),  
177 perturbation steps (PTB) as the step during which the perturbation was applied, and recovery  
178 steps (R<sub>1-3</sub>) as the three steps that followed the perturbation.

## 179 **2.5 Whole-body angular momentum**

180 We created a 13-segment, whole-body model in Visual3D and calculated the angular  
181 momentum of each segment about the body's center of mass for neurotypical participants (Herr  
182 & Popovic, 2008; Martelli et al., 2013). The model included the following segments: head,  
183 thorax, pelvis, upper arms, forearms, thighs, shanks, and feet. We modeled the limb segments'  
184 mass based on anthropometric tables (Dempster, 1955), and the segment geometry based on the  
185 description in Hanavan (Hanavan, 1964). For stroke participants, the pelvis segment was  
186 modeled to be rigidly connected to the trunk because they wore an extra harness that blocked the



187 markers necessary to track the pelvis accurately. Sagittal plane angular momentum was defined  
188 as the projection of angular momentum on the mediolateral axis passing through the body CoM  
189 (Silverman & Neptune, 2011). Whole-body angular momentum ( $L$ ) was computed as the sum of  
190 all segmental angular momenta which were composed of segmental rotation about the body's  
191 CoM and rotation of each segment about its CoM.  $L$  was nondimensionalized by a combination  
192 of the participant's mass ( $M$ ), the participant's height of COM ( $H$ ), and gravity constant ( $g$ ) to  
193 reduce between-subject variability (Eqn. 1)(Martelli et al., 2013).

$$L = \frac{\sum_i [ m_i ( \vec{r}_{CM-i}^i \times \vec{v}_{CM-i}^i ) + I^i \omega^i ]}{M g^{\frac{1}{2}} H^{\frac{3}{2}}} \quad (1)$$

194  
195 Here,  $m$  is segmental mass,  $r$  is the distance from segment to the body COM,  $I$  is the  
196 segmental moment of inertia,  $\omega$  is the segmental angular velocity, and the index  $i$  corresponds to  
197 individual limb segments. Negative values of angular momentum represented forward rotation,  
198 while positive values represented backward rotation. Although we used a 12-segment instead of  
199 a 13-segment model for people post-stroke, this had a negligible effect on whole-body angular  
200 momentum. The root-mean-square error for the peak backward and forward whole-body angular  
201 momentum in the sagittal plane between the 12-segment model and the 13-segment model was  
202  $2.1 \pm 1.5 \%$  and  $0.95 \pm 0.70 \%$ , respectively (Park et al., 2021). We computed integrated whole-  
203 body angular momentum ( $L_{int}$ ) for each step cycle to characterize changes in the body  
204 configuration over each step (Liu et al., 2018; Potocanac et al., 2014).

## 205 **2.6 Measures of reactive control strategies**

206 In addition to whole-body angular momentum, we used angular impulse to quantify the  
207 mechanical consequences of the reactive control strategies on whole-body dynamics. We

208 determined the effect of the ground reaction forces from each limb on the change in whole-body  
209 dynamics using measures of angular impulse as described in Eqn.2-3 (Figure 2). Similar to  
210 whole-body angular momentum, sagittal plane angular impulse was defined as the projection of  
211 angular impulse on the mediolateral axis passing through the body CoM. The earliest strategy  
212 that people could employ to begin recovering from losses of balance during the perturbation step  
213 is to modulate the ground reaction force of the perturbed limb to reduce the forward momentum  
214 about the CoM. Such a strategy is expected to occur no less than ~200ms after the onset of a  
215 perturbation and this would approach the late single-support phase of the gait cycle (Sloot et al.,  
216 2015). Thus, we first computed the forward pitch impulse ( $\Delta L_{\text{Stance}}$ ) during the late single support  
217 phase to capture the effect of the perturbed stance limb ground reaction force on whole-body  
218 dynamics (Eqn.2). The forward pitch impulse is mathematically equivalent to the change in  
219 whole-body angular momentum during the single support phase.

$$\Delta L_{\text{Stance}} = \int_{FS-\Delta t_s}^{FS} \vec{r}_s \times \vec{F}_s \, dt \quad (2)$$

220 Here,  $\vec{r}_s$  represents the displacement vector from the body's CoM to the center of  
221 pressure of the stance limb.  $\vec{F}_s$  represents the stance limb's ground reaction force. We defined the  
222 duration of the late single support phase ( $\Delta t_s$ ) as 80% of the average time from midstance to the  
223 subsequent foot strike during pre-perturbation steps. Midstance was defined as the midpoint  
224 between consecutive foot strikes during pre-perturbation steps. We used the same time duration  
225 across all step types to remove the effect of time on computing angular impulses. Index  $s$   
226 corresponds to the stance leg.

227 We also computed the net angular impulse ( $\Delta L_{\text{Net}}$ ) during the double support phase of the  
228 recovery step as the sum of the leading limb ( $\Delta L_{\text{Leading}}$ ) and trailing limb ( $\Delta L_{\text{Trailing}}$ ) angular

229 impulse (Eqn.3). The contributions to the net angular impulse from the leading and trailing limbs  
230 were computed similar to Eqn. 2, except that the integration was performed from foot-strike (FS)  
231 to FS +  $\Delta t_{ds}$ .  $\Delta t_{ds}$  represents the double support phase (Adamczyk & Kuo, 2009). We again  
232 used 80% of the average double support time during pre-perturbation steps so that the same  
233 duration was used across all step types.

$$\Delta L_{Net} = \Delta L_{Leading} + \Delta L_{Trailing} \quad (3)$$

## 234 **2.7 Statistical Analysis**

235 All statistical analyses were performed in Matlab 2020b (Mathworks). For people post-  
236 stroke, if the non-paretic leg was perturbed, the Pre-PTB step, PTP step, R<sub>2</sub>, and R<sub>4</sub> steps were  
237 non-paretic steps, and the R<sub>1</sub> and R<sub>3</sub> steps were paretic steps, and vice versa for the paretic  
238 perturbations.

239 We first tested whether there were significant differences in any participant  
240 characteristics between control and post-stroke participants by using a two-sample t-test with  
241 unequal variances. We also tested whether there were significant differences in  $L_{int}$ ,  $\Delta L_{stance}$ ,  
242  $\Delta L_{Net}$ ,  $\Delta L_{Leading}$ , and  $\Delta L_{Trailing}$  during the pre-perturbation step between the control and stroke  
243 group (paretic and non-paretic steps) and within the stroke group (paretic vs. non-paretic steps).  
244 We analyzed the normality of these measures using the Shapiro-Wilk Test. We used a two-  
245 sample unequal variance t-test if the data were normally distributed; otherwise, we used the  
246 Mann-Whitney test. We adjusted for multiple comparisons using Bonferroni corrections.

247 We then assessed if any of the dependent variables  $L_{int}$ ,  $\Delta L_{Net}$ ,  $\Delta L_{Leading}$ , and  $\Delta L_{Trailing}$   
248 following perturbations differed from those measured during the pre-perturbation step using  
249 linear mixed-effect models for stroke participants and control participants, respectively. The

250 independent variables for this analysis included Step Type (Pre-PTB<sub>1-2</sub>, PTB, R<sub>1-3</sub>), side of  
251 perturbation (Leg) (paretic and non-paretic side), and the interaction between Step Type and Leg  
252 to determine if changes in any of the dependent variables from the pre-perturbation step differed  
253 between sides. The reference level was set to be Pre-PTB<sub>1</sub>. For neurotypical participants, we did  
254 not find that any of the variables differed between sides. Thus, we combined values across limbs  
255 for the remainder of the analysis and the independent variable only included Step Type (Pre-  
256 PTB<sub>1-2</sub>, PTB, R<sub>1-3</sub>). We included a random intercept for each model to account for unmodeled  
257 sources of between-subject variability. We also determined the number of recovery steps needed  
258 for participants to restore balance by identifying when  $L_{int}$  returned to values measured before the  
259 perturbations. We analyzed the angular impulse during the perturbation and first recovery steps  
260 as our prior work demonstrated that reactive stabilization strategies were most evident during  
261 these two steps (Liu et al., 2018). We used the Shapiro-Wilk Test to test the residual normality.  
262 We provide detailed statistical results in Table S1 for this analysis.

263 We also determined if the deviation of the dependent variables from pre-perturbation  
264 values differed between neurotypical participants and stroke participants following paretic and  
265 non-paretic perturbations. We used a two-sample unequal variance t-test if the variables were  
266 normally distributed; otherwise, we used the Mann-Whitney test, and the comparisons between  
267 groups were adjusted for multiple comparisons using Bonferroni corrections. We provided  
268 detailed statistical results for this test of normality in Table S2. Lastly, we computed Pearson  
269 correlation coefficients to test for associations between changes in  $\Delta L_{stance}$  during the  
270 perturbation step, changes in  $\Delta L_{Leading}$  and  $\Delta L_{Trailing}$  during the first recovery step relative to the  
271 pre-perturbation step, and each clinical balance assessment (BBS, FGA, ABC, FM). Significance  
272 was set at  $\alpha = 0.05$ .

## 273 3 Results

### 274 3.1 Whole-body angular momentum

275 The acceleration of the belts caused consistent increases in forward angular momentum  
276 and triggered multi-step balance recovery responses for both neurotypical participants and  
277 people post-stroke (Figure 3, first row). During the perturbation step, angular momentum became  
278 more negative as the body rotated forward. To compensate for the perturbation, participants then  
279 generated positive angular momentum and initiated backward rotation during the first recovery  
280 step (Figure 3, first row). We also computed the integrated angular momentum over each step to  
281 characterize changes in body configuration in response to perturbations. Participants increased  
282 their forward rotation, indicated by a more negative  $L_{int}$ , during the perturbation step relative to  
283 the pre-perturbation step (Figure 4). They then countered the effects of the perturbation during  
284 the first recovery step ( $R_1$ ) as indicated by a more positive  $L_{int}$ . Neurotypical participants  
285 restored whole-body angular momentum to levels comparable to those observed during the pre-  
286 perturbation step by the second recovery step while people post-stroke restored angular  
287 momentum to pre-perturbation values by the third recovery step (Figure 4).

288 Stroke participants (36 out of 38) increased integrated angular momentum more during  
289 paretic perturbations relative to non-paretic perturbations ( $p = 0.021$ ), indicating that they fell  
290 forward more when the perturbation occurred during paretic stance. The increase in integrated  
291 angular momentum during the perturbation step was higher during paretic perturbations than for  
292 neurotypical participants (Bonferroni corrected  $p = 0.018$ ), but there was no difference in the  
293 increase in integrated angular momentum between non-paretic perturbations and those for  
294 neurotypical participants ( $p = 0.56$ ).

## 295 **3.2 Changes in the stance-phase forward pitch impulse during the perturbation**

### 296 **( $\Delta L_{\text{Stance}}$ )**

297 We did not observe any difference increase in forward pitch impulse between  
298 neurotypical participants and stroke participants during the perturbation step (Bonferroni  
299 corrected  $p > 0.05$ ) or any difference between limbs in people post-stroke ( $p = 0.088$ ). The earliest  
300 strategy that people could employ to begin recovering from losses of balance during the  
301 perturbation step is to modulate the ground reaction force of the perturbed limb to reduce the  
302 forward angular momentum about CoM. The ground reaction force produced by the stance limb  
303 from midstance to the subsequent foot strike typically produced a forward pitch impulse (Figure  
304 5A, Figure S1). During the perturbation step, neurotypical participants produced a smaller  
305 forward pitch impulse relative to the pre-perturbation step ( $p = 0.0005$ , Figure 6) indicating that  
306 they began to arrest the forward loss of balance during the perturbation step. However, people  
307 post-stroke only decreased the forward pitch impulse during non-paretic perturbations (29 out of  
308 38 participants,  $p = 0.005$ ) and not during paretic perturbations ( $p = 0.67$ , Figure 6). Although 30  
309 of 38 participants had greater reductions in forward pitch impulse during non-paretic  
310 perturbations compared to paretic perturbations, there was no significant difference between  
311 sides ( $p = 0.088$ ).

## 312 **3.3 Changes in the net angular impulse during the recovery step ( $\Delta L_{\text{Net}}$ )**

313 Neurotypical participants increased net angular impulse from the pre-perturbation step  
314 more than stroke participants during the double support phase of the first recovery step following  
315 paretic perturbations (Bonferroni corrected  $p = 0.0072$ ) but this increase did not differ from  
316 stroke participants following non-paretic perturbations (Bonferroni corrected  $p = 0.051$ ). For the

317 pre-perturbation step, the net angular impulse was typically positive during the double support  
318 phase for neurotypical individuals, indicating that the ground reaction forces by the leading and  
319 trailing limbs generated a net increase in backward angular momentum during this period (Figure  
320 S2A). During the first recovery step following a perturbation, neurotypical participants increased  
321 the net angular impulse ( $p < 0.0001$ , Figure 7A), which helped reduce the forward momentum  
322 generated by the perturbation. For people post-stroke, the net angular impulse during the first  
323 recovery step increased from the pre-perturbation step following non-paretic perturbations (27  
324 out of 38 participants,  $p = 0.0003$ ) but not following paretic perturbations ( $p = 0.1$ , Figure 7A).  
325 This result suggests that people post-stroke did not arrest the forward falls as completely when  
326 perturbations occurred on the paretic side.

#### 327 **3.4 Changes in the leading limb angular impulse during the recovery step ( $\Delta L_{\text{Leading}}$ )**

328 There was no difference in the increase in leading limb backward impulse during the first  
329 recovery step between stroke and neurotypical participants (All Bonferroni corrected  $p > 0.05$ ).  
330 During the pre-perturbation step, the ground reaction force generated by the leading leg of  
331 neurotypical control participants produced a backward angular impulse about the CoM during  
332 the double support phase (Figure 5D, Figure S2C). During the double support phase of the first  
333 recovery step, neurotypical participants increased this backward impulse to help arrest the  
334 forward fall, and this was evidenced by a more positive leading limb angular impulse for  
335 neurotypical participants ( $p < 0.0001$ , Figure 7B). For stroke participants, leading limb angular  
336 impulse increased from the pre-perturbation step following paretic perturbations (33 out of 38  
337 participants,  $p = 0.0006$ ) but not following non-paretic perturbations ( $p = 0.075$ , Figure 7B).

### 338 **3.5 Changes in the trailing limb angular impulse during the recovery step ( $\Delta L_{\text{Trailing}}$ )**

339 Neurotypical participants reduced trailing limb angular impulse more than stroke  
340 participants following paretic perturbations (Bonferroni corrected  $p = 0.0033$ ) but not following  
341 non-paretic perturbations (Bonferroni corrected  $p = 0.69$ ). Stroke participants also reduced  
342 forward trailing limb angular impulse more by the non-paretic limb following non-paretic  
343 perturbations than following paretic perturbations (29 out of 38 participants,  $p = 0.029$ ). During  
344 the pre-perturbation step, the ground reaction force by the trailing limb generated a forward  
345 moment about the body's CoM and thus the trailing limb angular impulse was negative for  
346 neurotypical participants (Figure 5G, Figure S2E). Neurotypical participants decreased their  
347 forward angular impulse which indicates that the trailing limb assisted with recovery from a  
348 forward loss of balance. During the first recovery step, forward trailing limb angular impulse did  
349 not change from the pre-perturbation step following non-paretic perturbations ( $p = 0.27$ ) for  
350 stroke participants. However, forward trailing limb angular impulse increased following paretic  
351 perturbations from the pre-perturbation step (21 out of 38 participants,  $p = 0.047$ ).

### 352 **3.6 Association between reactive stabilization strategies and clinical measures**

353 Lastly, we assessed whether changes in forward pitch impulse during the perturbation  
354 step, leading limb angular impulse during the first recovery step, and trailing limb angular  
355 impulse during the first recovery step from the pre-perturbation steps were associated with  
356 clinical assessment of balance and motor impairment (BBS, FGA, ABC, FM) in our sample of  
357 stroke participants. We found significant correlations between paretic trailing limb angular  
358 impulse and scores on clinical assessments of balance and motor impairment. The reduction in  
359 trailing limb angular impulse following the paretic perturbations relative to the pre-perturbation



360 step was positively correlated with FM ( $R^2= 0.31$ ,  $p = 0.0002$ ) and FGA ( $R^2= 0.23$ ,  $p = 0.002$ ,  
361 Figure 8). This indicated that participants who scored poorer on clinical assessments of balance  
362 and had greater motor impairment made less use of the paretic limb to reduce forward  
363 momentum.

#### 364 **4 Discussion**

365 The primary objective of this study was to determine how stroke affects the mechanical  
366 consequence of reactive control strategies in response to sudden treadmill accelerations. We  
367 found that perturbations to the paretic side led to more whole-body rotation during the  
368 perturbation step relative to non-paretic perturbations for people post-stroke and relative to  
369 neurotypical participants. To recover from these perturbations, neurotypical participants first  
370 used the perturbed stance limb to decrease the forward pitch impulse during the perturbed step.  
371 Then, during the double support phase of the first recovery step, they increased the leading limb  
372 angular impulse and decreased the forward trailing angular impulse by the perturbed limb  
373 relative to the pre-perturbation step. These reactive control strategies allowed neurotypical  
374 participants to restore the whole-body angular momentum to baseline levels within two steps.

375 In contrast to neurotypical participants, following paretic perturbations, people post-  
376 stroke did not decrease the forward angular impulse by the stance limb during the perturbed  
377 steps. People post-stroke also did not increase the leading limb angular impulse using the paretic  
378 leg or reduce the trailing limb angular impulse using their paretic leg during the double support  
379 phase of the first recovery step. However, when comparing responses to paretic versus non-  
380 paretic perturbations, we found that people post-stroke reduced their trailing limb angular  
381 impulse during the first recovery step more following non-paretic perturbations. Overall, people

382 post-stroke primarily relied on their non-paretic limb to restore balance in contrast to  
383 neurotypical individuals who generated responses with substantial contributions from both limbs.

384       People post-stroke required more recovery steps to restore whole-body angular  
385 momentum than neurotypical individuals. Studies investigating postural control have used the  
386 number of recovery steps to quantify people's ability to maintain balance in response to  
387 perturbation, and the use of multiple recovery steps is indicative of higher fall risk (Hilliard et  
388 al., 2008; Maki & McIlroy, 2006). For example, older adults, particularly those with a fall  
389 history, had a greater tendency to adopt multiple steps following a waist pull when standing  
390 compared to young adults (Mille et al., 2013). Additionally, people post-stroke needed more  
391 steps to restore balance following stance perturbations compared to age-matched controls  
392 (Martinez et al., 2019). Our results extended these observations to perturbations during walking  
393 by showing that people post-stroke needed one more recovery step following the treadmill-  
394 induced, slip-like perturbations to restore balance compared with age-matched neurotypical  
395 participants.

396       The increase in integrated whole-body angular momentum following paretic  
397 perturbations was higher than for non-paretic perturbations, indicating that people tended to fall  
398 forward more during paretic perturbations than non-paretic perturbations. The increase in the  
399 integrated whole-body angular momentum during the paretic perturbation step was about ~1.5  
400 times higher than that on the non-paretic side. The increase in whole-body angular momentum  
401 from the pre-perturbation step following paretic perturbations was also higher than that for  
402 neurotypical participants, indicating that people post-stroke have impaired regulation of whole-  
403 body dynamics following paretic perturbations, which is in line with prior work indicating

404 greater instability during backward losses of balance following paretic perturbations (Kajrolkar  
405 & Bhatt, 2016).

406 We observed marked differences in the mechanics of the most rapid balance correcting  
407 responses following paretic versus non-paretic perturbations. Neurotypical participants  
408 responded to the perturbations by modulating the stance limb ground reaction force toward the  
409 end of the perturbed steps to reduce forward angular impulse. However, at the group level, post-  
410 stroke participants did not reduce this impulse when the paretic limb was perturbed. This could  
411 be because the paretic perturbation steps were on average 145ms shorter than the non-paretic  
412 perturbation steps in our study. As a result, there might not be sufficient time for stroke  
413 participants to reduce the angular impulse during the stance phase during the paretic perturbation  
414 step. Additionally, people post-stroke may have delayed reactions to paretic perturbations due to  
415 sensory transmission or processing deficits, which would contribute to the increased forward loss  
416 of balance during paretic perturbations (Sharafi et al., 2016; C. Wutzke et al., 2013; C. J. Wutzke  
417 et al., 2015).

418 People post-stroke also showed impairments in the ability to increase leading limb  
419 angular impulse using the paretic limb relative to the non-paretic limb. Angular impulse is  
420 determined by the distance between the ground reaction force vectors the body's center mass,  
421 reaction force magnitudes, and time duration of the forces applied. Neurotypical individuals  
422 regulate their ground reaction force vectors so that the vectors intersect slightly above the CoM  
423 throughout the gait cycle (Gruben & Boehm, 2012; Maus et al., 2010). This control strategy was  
424 also evident in neurotypical participants during perturbations that were generated by stepping  
425 down from a camouflaged curb (Vielemeyer et al., 2019). The ground reaction force vector from  
426 the leading limb continued to be directed above the CoM to generate a backward moment about

427 the CoM to counteract the forward fall (Vielemeyer et al., 2019). However, this stabilization  
428 strategy of using ground reaction forces to control body dynamics may not be feasible in people  
429 post-stroke as the paretic limb may have limited ability to control force vector orientation  
430 relative to the center of mass compared to neurotypical participants (Boehm & Gruben, 2016;  
431 Rogers et al., 2004). Although people post-stroke can increase their step length to restore balance  
432 following a forward fall (Haarman et al., 2017), increasing step length may not be sufficient to  
433 change the leading limb angular impulse. We found no association between the increase in  
434 leading limb angular impulse during the first recovery step and the increase in step length or  
435 distance between foot placement and CoM (all  $p > 0.05$ ). Thus, generating sufficient leading limb  
436 angular impulse to arrest a forward loss of balance requires regulation of both ground reaction  
437 force and foot placement. Increasing paretic ground reaction force at the leading limb during the  
438 double support phase may generate high impact loading at the paretic limb and potentially cause  
439 knee collapse due to the weakness at the knee extensors. Thus, limiting the increase in leading  
440 limb impact angular impulse may be a protective mechanism for people post-stroke to avoid  
441 injury but additional study is needed to confirm this hypothesis.

442         Additionally, during the recovery step, people post-stroke did not reduce their paretic  
443 trailing limb angular impulse following the forward losses of balance to the same extent as they  
444 did with the non-paretic limb. At the beginning of the first recovery step, neurotypical  
445 participants reduced the forward angular impulse generated by the trailing limb, which likely  
446 limited the forward loss of balance caused by the sudden belt speed increase. One way to reduce  
447 the trailing limb forward angular impulse is by increasing the propulsive force in the anterior  
448 direction to generate a larger backward moment about the CoM if the moment arm is kept the  
449 same. The ability to increase the propulsive force requires the coordination of the hip flexor,

450 knee extensor, and ankle plantarflexor moments of the trailing limb (Debelle et al., 2020;  
451 Pijnappels et al., 2005). Such a strategy may not be feasible for people post-stroke as they  
452 typically have abnormal coordination patterns which could prevent them from generating higher  
453 propulsive force at the trailing limb and redirect the ground reaction force vectors relative to the  
454 center of mass to reduce the overall angular impulse at the paretic limb (Allen et al., 2014; Finley  
455 et al., 2008; Hsiao et al., 2015; Sánchez et al., 2017).

456 Overall, our findings have important implications for interventions aimed at improving  
457 reactive balance control for people post-stroke. Specifically, our results may inform the design of  
458 perturbation-based interventions that seek to improve reactive stepping responses. The increased  
459 disturbance caused by paretic perturbations may reflect an inability to direct the ground reaction  
460 force vector of the paretic leg correctly relative to the body center of mass to reduce the forward  
461 loss of balance. Moreover, during the subsequent recovery steps following the perturbations,  
462 people post-stroke primarily relied on their non-paretic limb instead of coordinating both limbs  
463 to restore balance. Thus, future studies may investigate whether training could improve the  
464 ability to modulate paretic force vectors relative to the body center of mass so that momentum  
465 can be properly regulated throughout the gait cycle.

#### 466 **4.1 Limitations**

467 In this current study protocol, we only elicited perturbations to induce forward loss of  
468 balance during walking with the same perturbation magnitudes for all participants. It remains to  
469 be determined if similar conclusions about the reactive stabilization strategies generated by  
470 people post-stroke extend to larger perturbations and perturbations in other directions. Moreover,  
471 although participants completed a familiarization trial to minimize the first trial effects, they may

472 have adopted proactive active strategies that they would not typically employ due to heightened  
473 certainty about the likelihood of an upcoming perturbation.

## 474 **5 Acknowledgments**

475 We thank Cathy Broderick, Catherine Yunis, Ryan Novotny, and Sungwoo Park for their  
476 help with data collection. This work was supported by the Eunice Kennedy Shriver National  
477 Institute of Child Health & Human Development of the National Institutes of Health under  
478 Award Number R01HD091184 and SC CTSI (NIH/NCATS) through Grant UL1TR001855.

## 479 **6 Author Contributions**

480 C.L collected the data, analyzed data, and wrote the manuscript. J.L.M advised in data  
481 analysis and edited the manuscript. J.M.F designed the experiment, advised in data analysis, and  
482 edited the manuscript.

## 483 **7 Conflict of Interest Statement**

484 The authors declare that the research was conducted in the absence of any commercial or  
485 financial relationships that could be construed as a potential conflict of interest.

## 486 **8 References**

487 Adamczyk, P. G., & Kuo, A. D. (2009). Redirection of center-of-mass velocity during the step-  
488 to-step transition of human walking. *Journal of Experimental Biology*, 212(16), 2668–  
489 2678. <https://doi.org/10.1242/jeb.027581>  
490 Allen, J. L., Kautz, S. A., & Neptune, R. R. (2014). Forward propulsion asymmetry is indicative  
491 of changes in plantarflexor coordination during walking in individuals with post-stroke

- 492 hemiparesis. *Clinical Biomechanics*, 29(7), 780–786.  
493 <https://doi.org/10.1016/j.clinbiomech.2014.06.001>
- 494 Arene, N., & Hidler, J. (2009). Understanding motor impairment in the paretic lower limb after a  
495 stroke: A review of the literature. *Topics in Stroke Rehabilitation*, 16(5), 346–356.  
496 <https://doi.org/10.1310/tsr1605-346>
- 497 Berg, K. O., Maki, B. E., Williams, J. I., Holliday, P. J., & Wood-Dauphinee, S. L. (1992).  
498 Clinical and laboratory measures of postural balance in an elderly population. *Archives of*  
499 *Physical Medicine and Rehabilitation*, 73(11), 1073–1080. [https://doi.org/0003-](https://doi.org/0003-9993(92)90174-U)  
500 9993(92)90174-U [pii]
- 501 Boehm, W. L., & Gruben, K. G. (2016). Post-Stroke Walking Behaviors Consistent with Altered  
502 Ground Reaction Force Direction Control Advise New Approaches to Research and  
503 Therapy. *Translational Stroke Research*, 7(1), 3–11. [https://doi.org/10.1007/s12975-015-](https://doi.org/10.1007/s12975-015-0435-5)  
504 0435-5
- 505 Buurke, T. J. W., Liu, C., Park, S., den Otter, R., & Finley, J. M. (2020). Maintaining sagittal  
506 plane balance compromises frontal plane balance during reactive stepping in people post-  
507 stroke. *Clinical Biomechanics*, 80, 105135.  
508 <https://doi.org/10.1016/j.clinbiomech.2020.105135>
- 509 Chen, G., Patten, C., Kothari, D. H., & Zajac, F. E. (2005). Gait differences between individuals  
510 with post-stroke hemiparesis and non-disabled controls at matched speeds. *Gait &*  
511 *Posture*, 22(1), 51–56. <https://doi.org/10.1016/j.gaitpost.2004.06.009>
- 512 Debelle, H., Harkness-Armstrong, C., Hadwin, K., Maganaris, C. N., & O'Brien, T. D. (2020).  
513 Recovery From a Forward Falling Slip: Measurement of Dynamic Stability and Strength

- 514 Requirements Using a Split-Belt Instrumented Treadmill. *Frontiers in Sports and Active*  
515 *Living*, 2, 82. <https://doi.org/10.3389/fspor.2020.00082>
- 516 Dempster, W. T. (1955). Space requirements of the seated operator: Geometrical, kinematic, and  
517 mechanical aspects other body with special reference to the limbs. In *WADC Technical*  
518 *Report* (pp. 1–254). <https://doi.org/AD 087892>
- 519 Dusane, S., Gangwani, R., Patel, P., & Bhatt, T. (2021). Does stroke-induced sensorimotor  
520 impairment and perturbation intensity affect gait-slip outcomes? *Journal of*  
521 *Biomechanics*, 118, 110255. <https://doi.org/10.1016/j.jbiomech.2021.110255>
- 522 Finley, J. M., Perreault, E. J., & Dhaher, Y. Y. (2008). Stretch reflex coupling between the hip  
523 and knee: Implications for impaired gait following stroke. *Experimental Brain Research*,  
524 188(4), 529–540. <https://doi.org/10.1007/s00221-008-1383-z>
- 525 Fugl-Meyer, A. R., Jääskö, L., Leyman, I., Olsson, S., & Steglind, S. (1975). The post-stroke  
526 hemiplegic patient. 1. A method for evaluation of physical performance. *Scandinavian*  
527 *Journal of Rehabilitation Medicine*, 7(1), 13–31. <https://doi.org/10.1038/35081184>
- 528 Golyski, P. R., Vazquez, E., Leestma, J. K., & Sawicki, G. S. (2022). Onset timing of treadmill  
529 belt perturbations influences stability during walking. *Journal of Biomechanics*, 130,  
530 110800. <https://doi.org/10.1016/j.jbiomech.2021.110800>
- 531 Gruben, K. G., & Boehm, W. L. (2012). Force direction pattern stabilizes sagittal plane  
532 mechanics of human walking. *Human Movement Science*, 31(3), 649–659.  
533 <https://doi.org/10.1016/j.humov.2011.07.006>
- 534 Haarman, J. A. M., Vlutters, M., Olde Keizer, R. A. C. M., Van Asseldonk, E. H. F., Buurke, J.  
535 H., Reenalda, J., Rietman, J. S., & Van Der Kooij, H. (2017). Paretic versus non-paretic  
536 stepping responses following pelvis perturbations in walking chronic-stage stroke



- 537 survivors. *Journal of NeuroEngineering and Rehabilitation*, 14(1).  
538 <https://doi.org/10.1186/s12984-017-0317-z>
- 539 Hanavan, E. P. (1964). A Mathematical Model of the human body. *Aerospace Medical Research*  
540 *Laboratories*, 1–149.
- 541 Havens, K. L., Mukherjee, T., & Finley, J. M. (2018). Analysis of biases in dynamic margins of  
542 stability introduced by the use of simplified center of mass estimates during walking and  
543 turning. *Gait & Posture*, 59(June 2017), 162–167.  
544 <https://doi.org/10.1016/j.gaitpost.2017.10.002>
- 545 Herr, H. M., & Popovic, M. (2008). Angular momentum in human walking. *The Journal of*  
546 *Experimental Biology*, 211(4), 467–481. <https://doi.org/10.1242/jeb.008573>
- 547 Higginson, J. S., Zajac, F. E., Neptune, R. R., Kautz, S. A., & Delp, S. L. (2006). Muscle  
548 contributions to support during gait in an individual with post-stroke hemiparesis.  
549 *Journal of Biomechanics*, 39, 1769–1777. <https://doi.org/10.1016/j.jbiomech.2005.05.032>
- 550 Hilliard, M. J., Martinez, K. M., Janssen, I., Edwards, B., Mille, M. L., Zhang, Y., & Rogers, M.  
551 W. (2008). Lateral Balance Factors Predict Future Falls in Community-Living Older  
552 Adults. *Archives of Physical Medicine and Rehabilitation*, 89(9), 1708–1713.  
553 <https://doi.org/10.1016/j.apmr.2008.01.023>
- 554 Honda, K., Sekiguchi, Y., Muraki, T., & Izumi, S. I. (2019). The differences in sagittal plane  
555 whole-body angular momentum during gait between patients with hemiparesis and  
556 healthy people. *Journal of Biomechanics*, 86, 204–209.  
557 <https://doi.org/10.1016/j.jbiomech.2019.02.012>

- 558 Hsiao, H., Knarr, B. A., Higginson, J. S., & Binder-Macleod, S. A. (2015). The relative  
559 contribution of ankle moment and trailing limb angle to propulsive force during gait.  
560 *Human Movement Science*, 39, 212–221. <https://doi.org/10.1016/J.HUMOV.2014.11.008>
- 561 Kajrolkar, T., & Bhatt, T. (2016). Falls-risk post-stroke: Examining contributions from paretic  
562 versus non paretic limbs to unexpected forward gait slips. *Journal of Biomechanics*,  
563 49(13), 2702–2708. <https://doi.org/10.1016/j.jbiomech.2016.06.005>
- 564 Kajrolkar, T., Yang, F., Pai, Y.-C. Y.-C., & Bhatt, T. (2014). Dynamic stability and  
565 compensatory stepping responses during anterior gait-slip perturbations in people with  
566 chronic hemiparetic stroke. *Journal of Biomechanics*, 47(11), 2751–2758.  
567 <https://doi.org/10.1016/j.jbiomech.2014.04.051>
- 568 Kirker, S. G. B., Simpson, D. S., Jenner, J. R., & Wing, A. M. (2000). Stepping before standing:  
569 Hip muscle function in stepping and standing balance after stroke. *J Neurol Neurosurg*  
570 *Psychiatry*, 68, 458–464.
- 571 Kurz, M. J., Arpin, D. J., & Corr, B. (2012). Differences in the dynamic gait stability of children  
572 with cerebral palsy and typically developing children. *Gait and Posture*, 36(3), 600–604.  
573 <https://doi.org/10.1016/j.gaitpost.2012.05.029>
- 574 Lauzière, S., Miéville, C., Betschart, M., Aissaoui, R., & Nadeau, S. (2015). Plantarflexor  
575 weakness is a determinant of kinetic asymmetry during gait in post-stroke individuals  
576 walking with high levels of effort. *Clinical Biomechanics*, 30(9), 946–952.  
577 <https://doi.org/10.1016/j.clinbiomech.2015.07.004>
- 578 Leddy, A. L., Crowner, B. E., & Earhart, G. M. (2011). Functional gait assessment and balance  
579 evaluation system test: Reliability, validity, sensitivity, and specificity for identifying

- 580 individuals with Parkinson disease who fall. *Physical Therapy*, 91(1), 102–113.
- 581 <https://doi.org/10.2522/ptj.20100113>
- 582 Liu, C., De Macedo, L., & Finley, M. J. (2018). Conservation of Reactive Stabilization Strategies  
583 in the Presence of Step Length Asymmetries during Walking. *Frontiers in Human*  
584 *Neuroscience*, 12, 251. <https://doi.org/doi:10.3389/fnhum.2018.00251>
- 585 Maki, B. E., & McIlroy, W. E. (2006). Control of rapid limb movements for balance recovery:  
586 Age-related changes and implications for fall prevention. *Age and Ageing*, 35(SUPPL.2).  
587 <https://doi.org/10.1093/ageing/afl078>
- 588 Marigold, D. S., Eng, J. J., & Timothy Inglis, J. (2004). Modulation of ankle muscle postural  
589 reflexes in stroke: Influence of weight-bearing load. *Clinical Neurophysiology*, 115(12),  
590 2789–2797. <https://doi.org/10.1016/j.clinph.2004.07.002>
- 591 Martelli, D., Monaco, V., Bassi Luciani, L., Micera, S., Luciani, L. B., & Micera, S. (2013).  
592 Angular Momentum During Unexpected Multidirectional Perturbations Delivered While  
593 Walking. *IEEE Transactions on Biomedical Engineering*, 60(7), 1785–1795.  
594 <https://doi.org/10.1109/TBME.2013.2241434>
- 595 Martinez, K. M., Rogers, M. W., Blackinton, M. T., Samuel Cheng, M., & Mille, M. L. (2019).  
596 Perturbation-Induced Stepping Post-stroke: A pilot study demonstrating altered strategies  
597 of both legs. *Frontiers in Neurology*, 10(JUL). <https://doi.org/10.3389/fneur.2019.00711>
- 598 Mathiyakom, W., & McNitt-Gray, J. L. (2008). Regulation of angular impulse during fall  
599 recovery. In *Journal of Rehabilitation Research and Development*.  
600 <https://doi.org/10.1682/JRRD.2008.02.0033>

- 601 Maus, H. M., Lipfert, S. W., Gross, M., Rummel, J., & Seyfarth, A. (2010). Upright human gait  
602 did not provide a major mechanical challenge for our ancestors. *Nature Communications*,  
603 *1*(6). <https://doi.org/10.1038/ncomms1073>
- 604 Mille, M. L., Johnson-Hilliard, M., Martinez, K. M., Zhang, Y., Edwards, B. J., & Rogers, M.  
605 W. (2013). One step, two steps, three steps more... Directional vulnerability to falls in  
606 community-dwelling older people. *Journals of Gerontology - Series A Biological*  
607 *Sciences and Medical Sciences*, *68*(12 A), 1540–1548.  
608 <https://doi.org/10.1093/gerona/glt062>
- 609 Nott, C. R., Neptune, R. R., & Kautz, S. A. (2014). Relationships between frontal-plane angular  
610 momentum and clinical balance measures during post-stroke hemiparetic walking. *Gait*  
611 *& Posture*, *39*(1), 129–134. <https://doi.org/doi:10.1016/j.gaitpost.2013.06.008>.
- 612 Olney, S. J., & Richards, C. (1996). Hemiparetic gait following stroke. Part 1: Characteristics.  
613 *Gait & Posture*, *4*, 136–148. [https://doi.org/10.1016/0966-6362\(96\)01063-6](https://doi.org/10.1016/0966-6362(96)01063-6)
- 614 Park, S., Liu, C., Sánchez, N., Tilson, J. K., Mulroy, S. J., & Finley, J. M. (2021). Using  
615 Biofeedback to Reduce Step Length Asymmetry Impairs Dynamic Balance in People  
616 Poststroke. *Neurorehabilitation and Neural Repair*, *35*(8), 738–749.  
617 <https://doi.org/10.1177/15459683211019346>
- 618 Patel, P. J., & Bhatt, T. (2017). Fall risk during opposing stance perturbations among healthy  
619 adults and chronic stroke survivors. *Experimental Brain Research*, *1*(236), 619–628.  
620 <https://doi.org/10.1007/s00221-017-5138-6>
- 621 Pijnappels, M., Bobbert, M. F., & Dieën, J. H. van. (2005). Push-off reactions in recovery after  
622 tripping discriminate young subjects, older non-fallers and older fallers. *Gait & Posture*,  
623 *21*(4), 388–394. <https://doi.org/10.1016/j.gaitpost.2004.04.009>

- 624 Potocanac, Z., de Bruin, J., van der Veen, S., Verschueren, S., van Dieën, J., Duysens, J., &  
625 Pijnappels, M. (2014). Fast online corrections of tripping responses. *Experimental Brain*  
626 *Research*, 232(11), 3579–3590. <https://doi.org/10.1007/s00221-014-4038-2>
- 627 Powell, L. E., & Myers, A. M. (1995). The Activities-specific Balance Confidence (ABC) Scale.  
628 *The Journals of Gerontology: Series A: Biological Sciences and Medical Sciences*, 50(1),  
629 M28–M34. <https://doi.org/10.1093/gerona/50A.1.M28>
- 630 Reisman, D. S., Wityk, R., Silver, K., Bastian, A. J., & Manuscript, A. (2009). Split-Belt  
631 Treadmill Adaptation Transfers to Overground Walking in Persons Poststroke. *Physical*  
632 *Therapy*, 23(7), 735–744. <https://doi.org/10.1177/1545968309332880.Split-Belt>
- 633 Roeles, S., Rowe, P. J., Bruijn, S. M., Childs, C. R., Tarfali, G. D., Steenbrink, F., & Pijnappels,  
634 M. (2018). Gait stability in response to platform, belt, and sensory perturbations in young  
635 and older adults. *Medical & Biological Engineering & Computing*, 56(12), 2325–2335.  
636 <https://doi.org/10.1007/s11517-018-1855-7>
- 637 Roerdink, M., Geurts, A. C. H., de Haart, M., & Beek, P. J. (2009). On the Relative Contribution  
638 of the Paretic Leg to the Control of Posture After Stroke. *Neurorehabilitation and Neural*  
639 *Repair*, 23(3), 267–274. <https://doi.org/10.1177/1545968308323928>
- 640 Rogers, L. M., Brown, D. A., & Gruben, K. G. (2004). Foot force direction control during leg  
641 pushes against fixed and moving pedals in persons post-stroke. *Gait and Posture*, 19(1),  
642 58–68. [https://doi.org/10.1016/S0966-6362\(03\)00009-2](https://doi.org/10.1016/S0966-6362(03)00009-2)
- 643 Rybar, M. M., Walker, E. R., Kuhnen, H. R., Ouellette, D. R., Berrios, R., Hunter, S. K., &  
644 Hyngstrom, A. S. (2014). The stroke-related effects of hip flexion fatigue on over ground  
645 walking. *Gait and Posture*, 39(4), 1103–1108.  
646 <https://doi.org/10.1016/j.gaitpost.2014.01.012>

- 647 Salot, P., Patel, P., & Bhatt, T. (2016). Reactive Balance in Individuals With Chronic Stroke:  
648 Biomechanical Factors Related to Perturbation-Induced Backward Falling. *Physical*  
649 *Therapy*, 96(3), 338–347. <https://doi.org/10.2522/ptj.20150197>
- 650 Sánchez, N., Acosta, A. M., Lopez-Rosado, R., Stienen, A. H. A. ;, & Dewald, J. P. A. ; (2017).  
651 Lower Extremity Motor Impairments in Ambulatory Chronic Hemiparetic Stroke:  
652 Evidence for Lower Extremity Weakness and Abnormal Muscle and Joint Torque  
653 Coupling Patterns. *Neurorehabilitation and Neural Repair*, 31(9), 814–826.  
654 <https://doi.org/10.1177/1545968317721974>
- 655 Schmid, A. A., Yaggi, H. K., Burrus, N., McClain, V., Austin, C., Ferguson, J., Fragoso, C.,  
656 Sico, J. J., Miech, E. J., Matthias, M. S., Williams, L. S., & Bravata, D. M. (2013).  
657 Circumstances and consequences of falls among people with chronic stroke. *Journal of*  
658 *Rehabilitation Research and Development*, 50(9), 1277–1286.  
659 <https://doi.org/10.1682/JRRD.2012.11.0215>
- 660 Sharafi, B., Hoffmann, G., Tan, A. Q., & Y. Dhaher, Y. (2016). Evidence of impaired  
661 neuromuscular responses in the support leg to a destabilizing swing phase perturbation in  
662 hemiparetic gait. *Experimental Brain Research*, 234(12), 3497–3508.  
663 <https://doi.org/10.1007/s00221-016-4743-0>
- 664 Silverman, A. K., & Neptune, R. R. (2011). Differences in whole-body angular momentum  
665 between below-knee amputees and non-amputees across walking speeds. *Journal of*  
666 *Biomechanics*, 44(3), 379–385. <https://doi.org/10.1016/j.jbiomech.2010.10.027>
- 667 Sloot, L. H., Van Den Noort, J. C., Van Der Krogt, M. M., Bruijn, S. M., & Harlaar, J. (2015).  
668 Can treadmill perturbations evoke stretch reflexes in the calf muscles? *PLoS ONE*,  
669 10(12). <https://doi.org/10.1371/journal.pone.0144815>

- 670 Song, J., Sigward, S., Fisher, B., & Salem, G. J. (2012). Altered dynamic postural control during  
671 step turning in persons with early-stage Parkinson's disease. *Parkinson's Disease*, 2012,  
672 386962. <https://doi.org/10.1155/2012/386962>
- 673 Vielemeyer, J., Griebach, E., & Müller, R. (2019). Ground reaction forces intersect above the  
674 center of mass even when walking down visible and camouflaged curbs. *Journal of*  
675 *Experimental Biology*, 222(14). <https://doi.org/10.1242/jeb.204305>
- 676 Vlutters, M., Van Asseldonk, E. H. F., & Van Der Kooij, H. (2016). Center of mass velocity-  
677 based predictions in balance recovery following pelvis perturbations during human  
678 walking. *Journal of Experimental Biology*, 219(10), 1514–1523.  
679 <https://doi.org/10.1242/jeb.129338>
- 680 Weerdesteyn, V., De Niet, M., van Duijnhoven, H. J. R. R., Geurts, A. C. H. H., Niet, M. de, van  
681 Duijnhoven, H. J. R. R., & Geurts, A. C. H. H. (2008). Falls in individuals with stroke.  
682 *The Journal of Rehabilitation Research and Development*, 45(8), 1195.  
683 <https://doi.org/10.1682/JRRD.2007.09.0145>
- 684 Winter, D. A. (2009). Biomechanics and Motor Control of Human Movement. In *Motor Control*  
685 (Vol. 2nd). <https://doi.org/10.1002/9780470549148>
- 686 Wutzke, C. J., Faldowski, R. A., & Lewek, M. D. (2015). Individuals Poststroke Do Not  
687 Perceive Their Spatiotemporal Gait Asymmetries as Abnormal. *Physical Therapy*, 95(9),  
688 1244–1253. <https://doi.org/10.2522/ptj.20140482>
- 689 Wutzke, C., Mercer, V., & Lewek, M. (2013). Influence of lower extremity sensory function on  
690 locomotor adaptation following stroke: A review. *Topics in Stroke Rehabilitation*, 20(3),  
691 233–240. <https://doi.org/10.1310/tsr2003-233>  
692

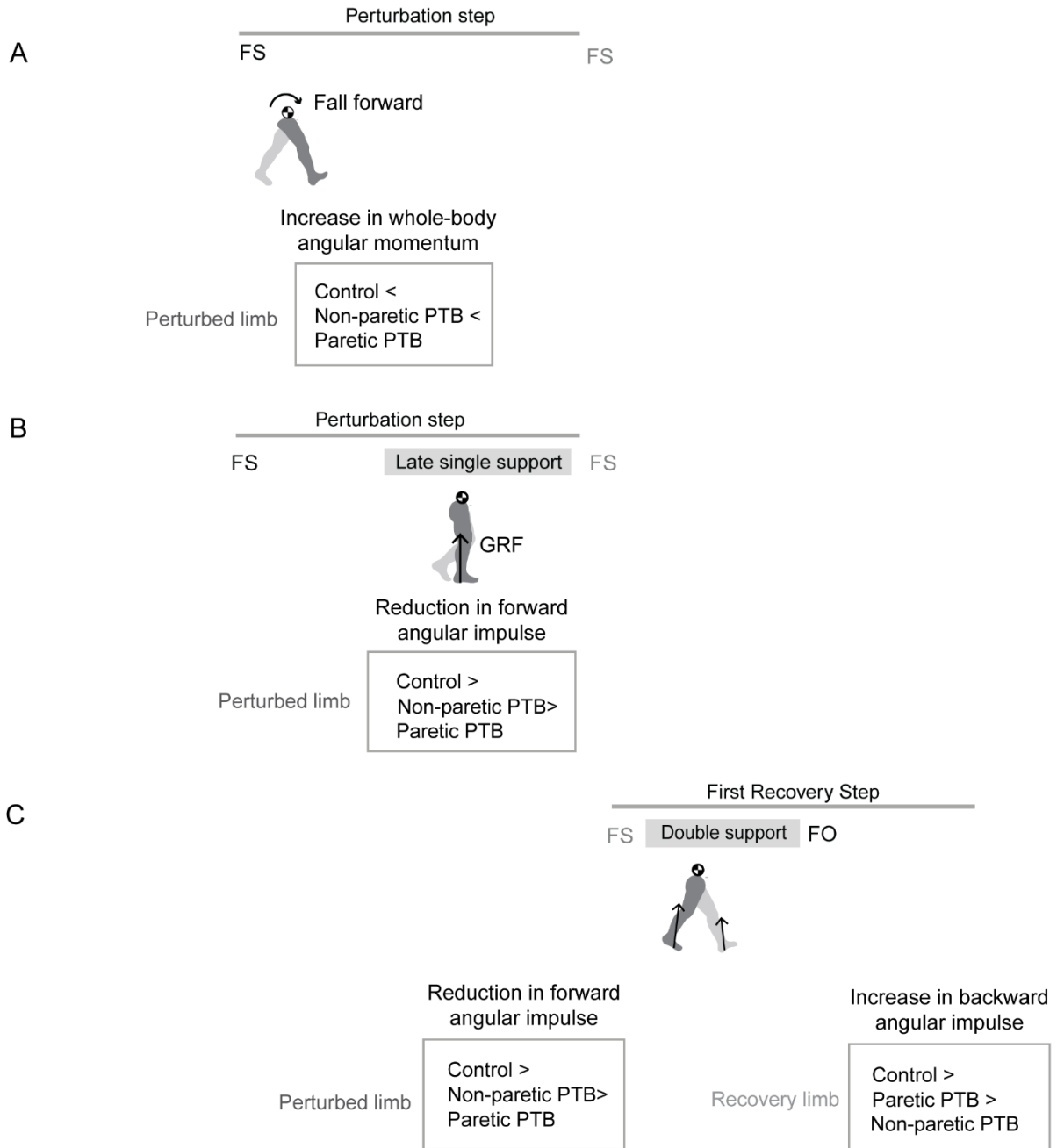
693 Table 1 Participant demographics for both control and stroke participants. Values are formatted  
 694 as Mean (SD).

	<b>Control (N = 13)</b>	<b>Stroke (N= 38)</b>	<b>p value</b>
Age (yrs)	58 (29)	60 (11)	0.76
Female/Male	6/7	14/24	/
Mass (kg)	76 (15)	81 (19)	0.38
Height of CoM (m)	0.97 (0.05)	0.94 (0.06)	0.13
Treadmill speed (m/s)	Matched: 0.6 (0.2)	0.6 (0.2)	0.62
Scaling factor $\sqrt{gL}$ (m/s)	3.08 (0.082)	3.04 (0.095)	0.13
Self-selected Overground speed (m/s)	1.3 (0.2)	0.8 (0.3)	<0.0001
Berg Balance Scale	55 (2)	51 (6)	0.017
Activity-specific Balance Confidence Scale	97 (3.5)	77 (13)	<0.0001
Falls Efficacy Scale	18 (2)	29 (12)	0.0025
Lower Extremity Fugl-Meyer	/	26 (5)	/
Left/right hemiparetic	/	15/23	/
Months after stroke	/	83 (55)	/
Functional Gait Assessment	/	21 (6)	/

695

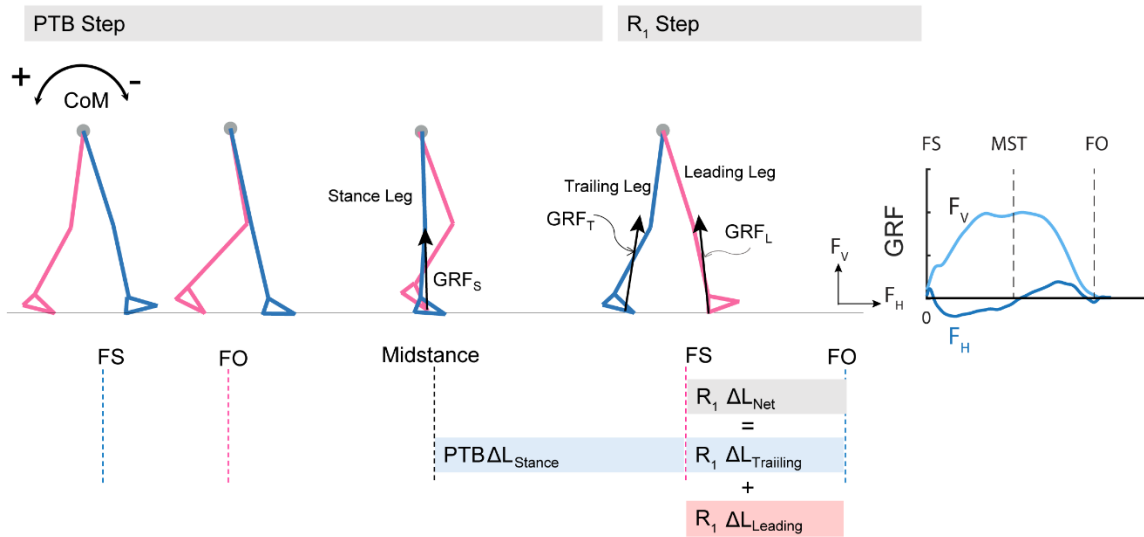
696





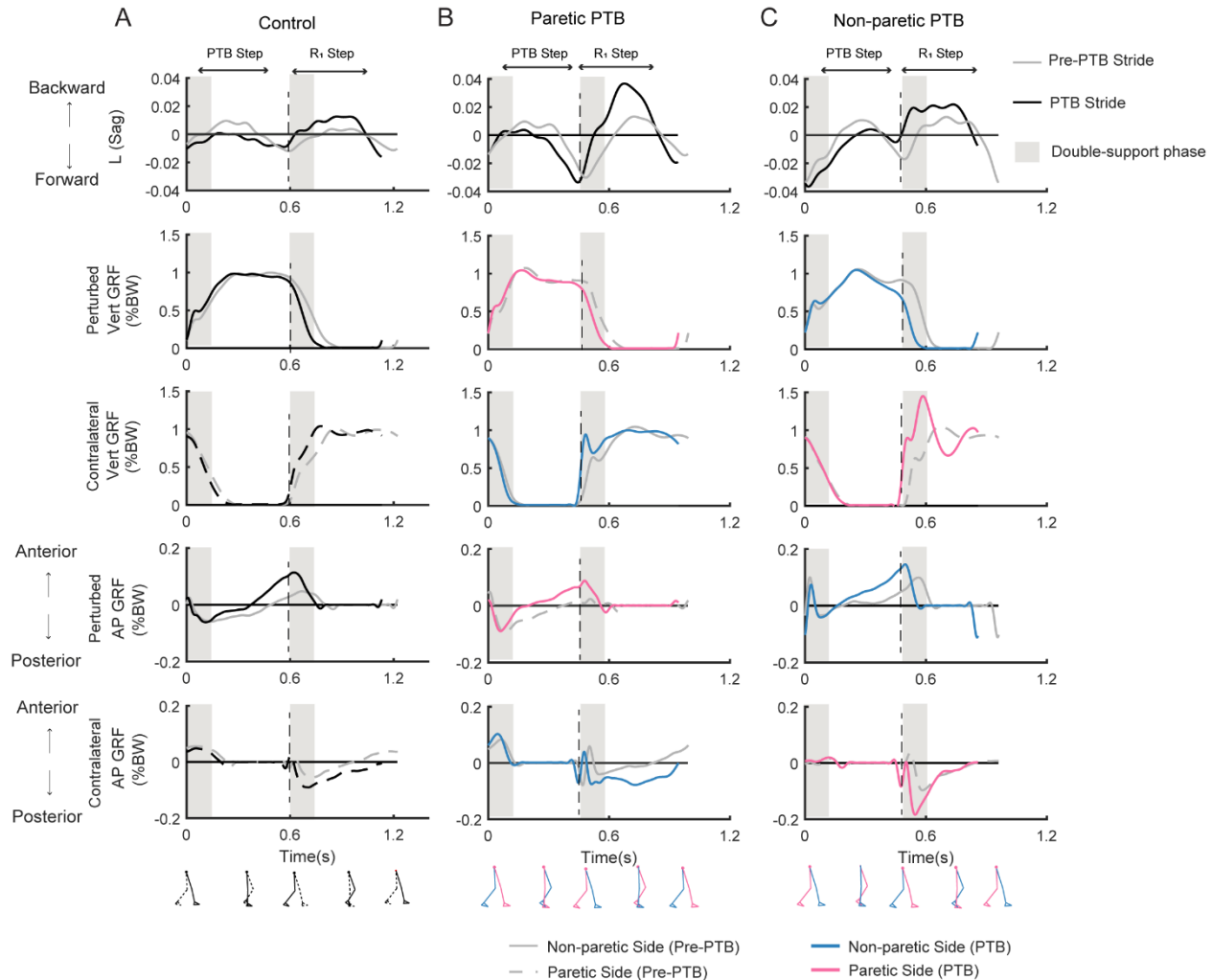
697  
698  
699  
700  
701  
702  
703  
704  
705  
706  
707

Figure 1: Graphical illustration of hypothesized differences in whole-body angular momentum and angular impulses. (A) Hypothesis for changes in whole-body angular momentum during the perturbation step and the first recovery step relative to that measured during the pre-perturbation step. (B) Hypothesis for changes in angular impulse during the late single support phase of the perturbation step relative to that measured during the pre-perturbation step. (C) Hypothesis for changes in the trailing perturbed limb angular impulse and the leading limb angular impulse during the double support phase of the first recovery step relative to that measured during the pre-perturbation step. (FS: foot strike; FO: foot-off; GRF: ground reaction force; PTB: perturbation)



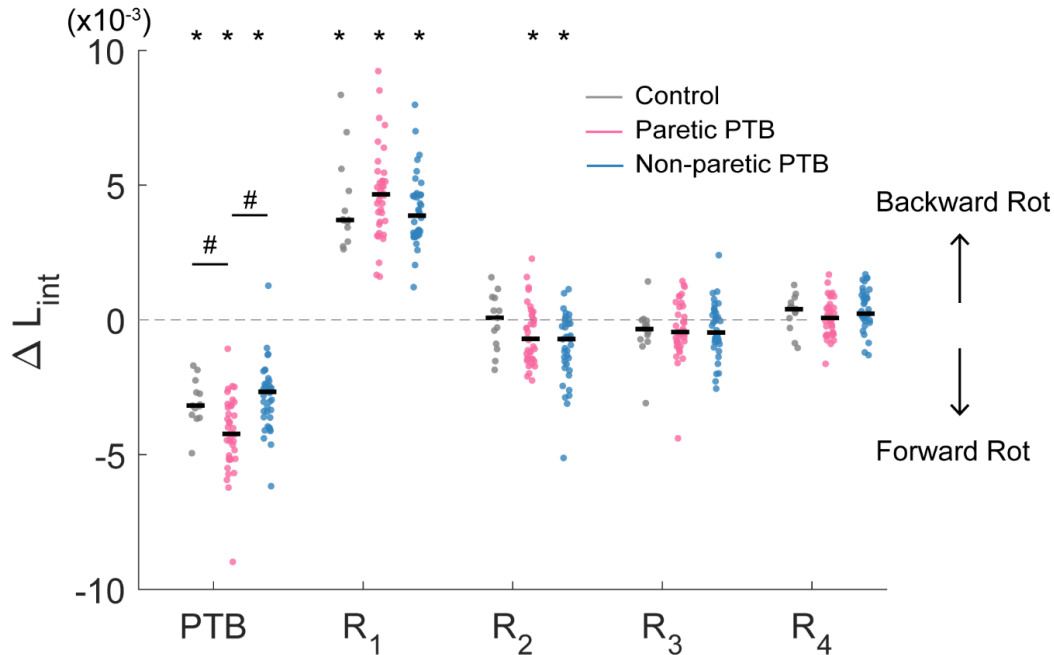
708  
709  
710  
711  
712  
713  
714  
715  
716  
717  
718  
719

Figure 2: Diagram of computed angular impulse about the body CoM by the leading and trailing leg during the perturbation (PTB) step and the first recovery step (R<sub>1</sub>) and illustration of ground reaction force from foot-strike to foot-off during one example perturbation step. The forward pitch impulse (PTB  $\Delta L_{Stance}$ ) is computed during the phase from midstance of the PTB step until the foot strike of the R<sub>1</sub> step. Net angular impulse ( $R_1 \Delta L_{Net}$ ) is computed as the sum of trailing limb angular impulse ( $R_1 \Delta L_{Trailing}$ ) and leading limb angular impulse ( $R_1 \Delta L_{Leading}$ ) during the double support phase of the R<sub>1</sub> step. FS: Foot strike; FO: Foot-off. The arrows (+/-) indicate the backward and forward moments by the GRF about CoM, respectively. F<sub>V</sub>: vertical ground reaction force; F<sub>H</sub>: fore-aft ground reaction force.



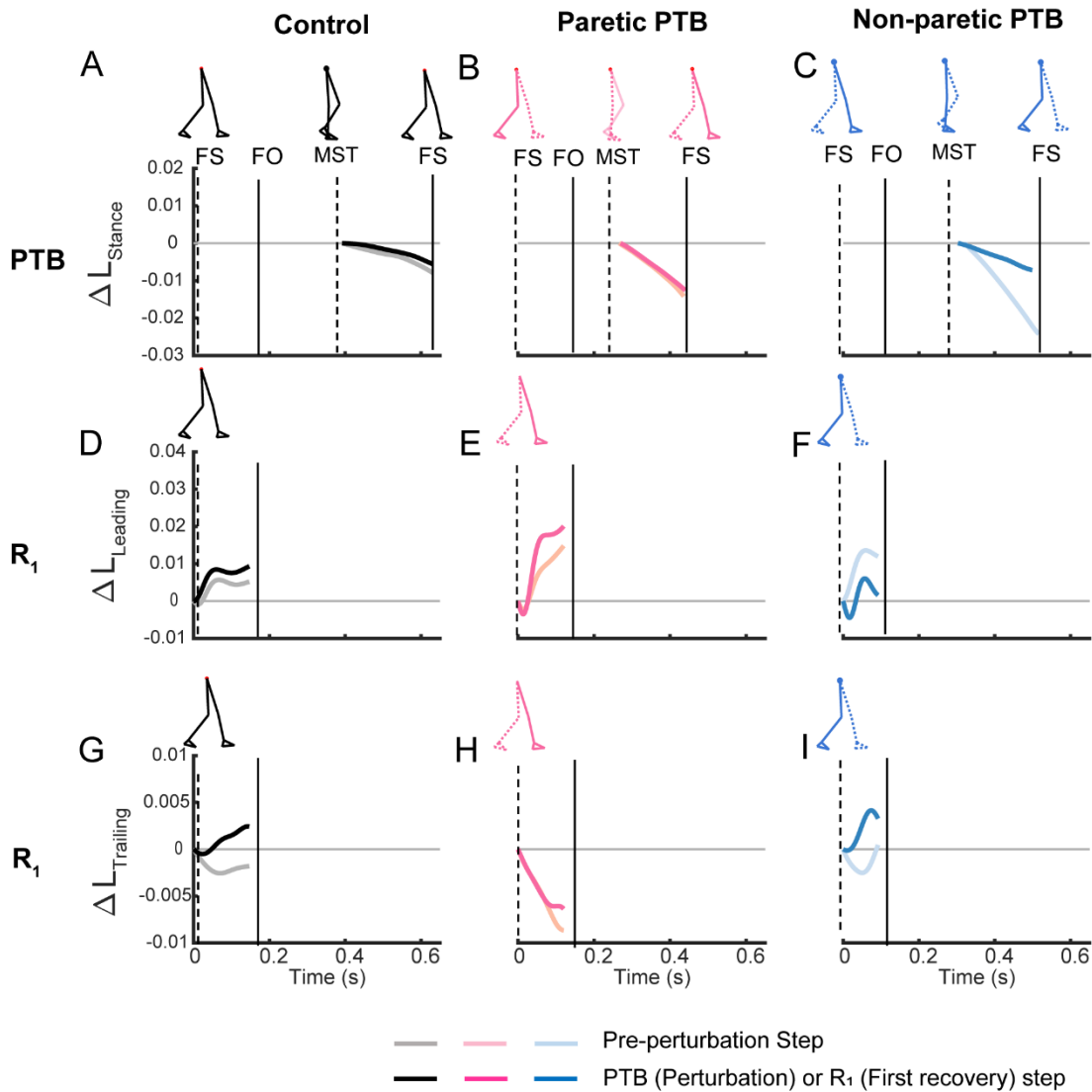
720  
 721 Figure 3: Whole-body angular momentum in the sagittal plane and ground reaction forces for  
 722 one representative neurotypical participant (A) and a stroke participant during a paretic  
 723 perturbation (B) and non-paretic perturbation (C) for both a pre-perturbation stride and a  
 724 perturbation stride. Each stride began at foot strike. The gray traces indicate the time series data  
 725 for a pre-perturbation stride while the black or colored traces indicate a perturbation stride.  
 726 Negative values of angular momentum represent forward rotation while positive values represent  
 727 backward rotation. Ground reaction forces (% body weight) in the vertical and anterior-posterior  
 728 directions for the perturbed and the contralateral limb when perturbations occurred on the  
 729 dominant side for the neurotypical participant (A), or on the paretic (B) or non-paretic sides (C)  
 730 for the stroke participant. For the neurotypical participant, black lines indicated the perturbed  
 731 side, and the dashed lines indicated the contralateral side. For the stroke participant, pink and  
 732 blue lines represent the paretic leg and non-paretic leg, respectively. Black dashed vertical lines  
 733 correspond to the time of foot strike. Gray shaded vertical box corresponds to the double support  
 734 phase from the time of foot strike to the contralateral foot-off. Pre-PTB: pre-perturbation stride;  
 735 PTB: perturbation stride.

736  
 737

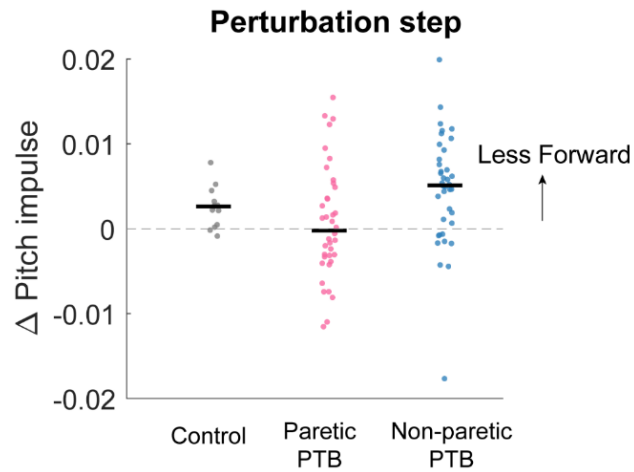


738  
739

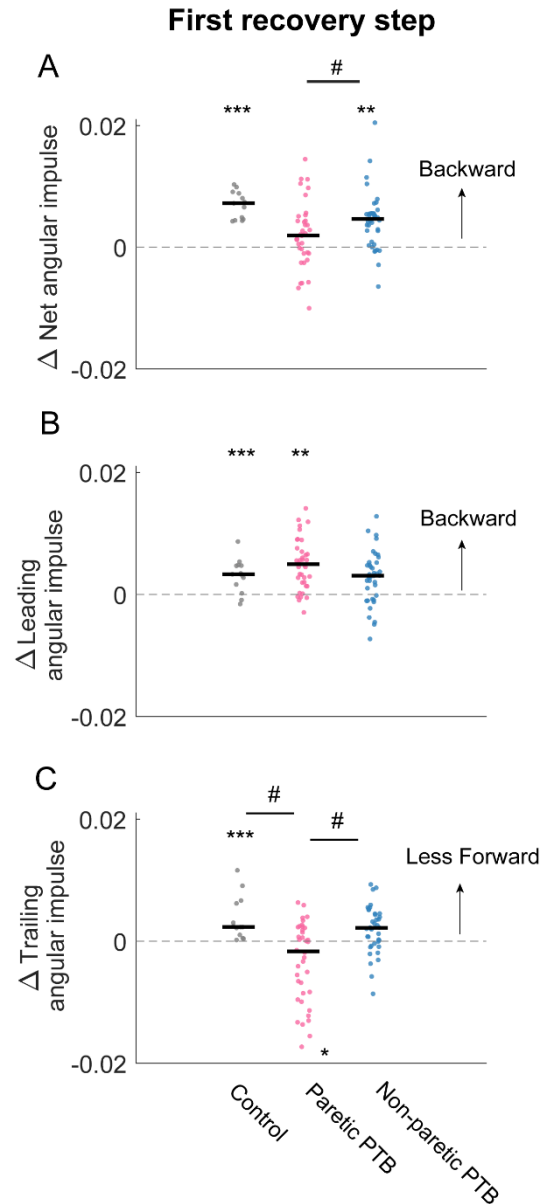
740 Figure 4. Median integrated angular momentum in the sagittal plane over the step cycle relative  
741 to the corresponding pre-perturbation step ( $\Delta L_{int}$ ) for all participants ( $N = 38$  stroke participants  
742 and  $N = 13$  neurotypical participants). Each dot represents one participant. Black horizontal lines  
743 indicate the median across participants. Steps alternated between paretic and non-paretic for  
744 stroke participants. PTB: Perturbation step; R: Recovery step. The asterisks on top of the  
745 boxplots indicate whether the difference in  $L_{int}$  from the pre-perturbation step was significantly  
746 different from zero ( $*p < 0.05$ ) and the # indicated that the  $\Delta L_{int}$  was different between groups.  
747 Note that for people post-stroke, if the non-paretic leg was perturbed, the R<sub>1</sub> steps were paretic,  
748 and Pre-PTB steps and PTB steps were non-paretic and vice versa for the paretic perturbations.  
749



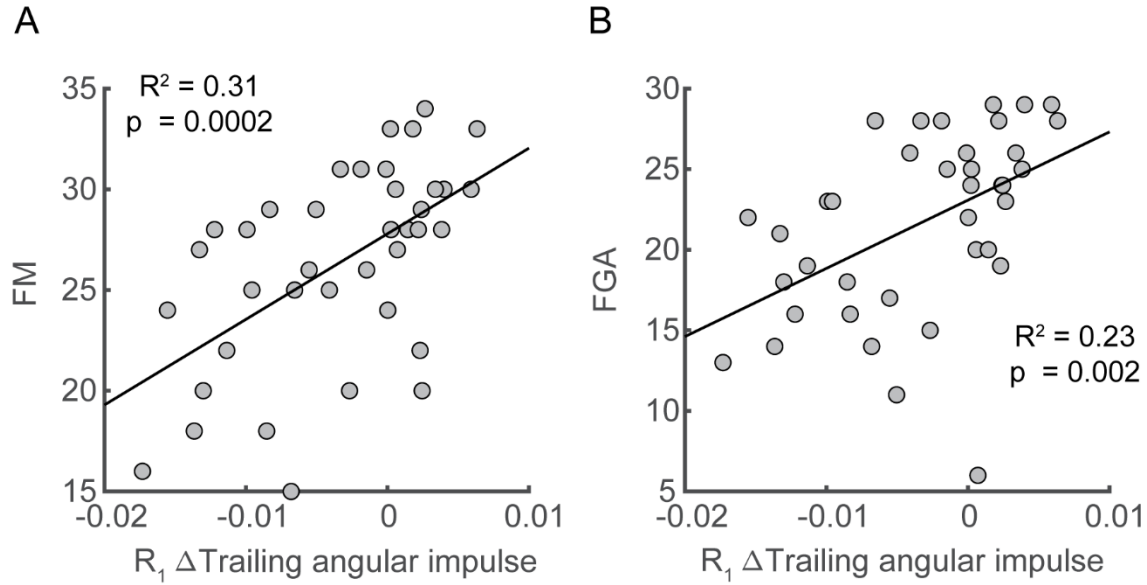
750  
 751 Figure 5. Time series trajectories of the PTB  $\Delta L_{Stance}$ ,  $R_1 \Delta L_{Leading}$ ,  $R_1 \Delta L_{Trailing}$ , and the  
 752 corresponding trajectories during the pre-perturbation step for a representative neurotypical  
 753 perturbation (left), one paretic perturbation (middle), and one non-paretic perturbation (right).  
 754 Pre-perturbation trajectories are shown in lighter colors while perturbation and recovery traces  
 755 are shown in darker colors. The first, second, and third rows correspond to PTB  $\Delta L_{Stance}$ ,  $R_1$   
 756  $\Delta L_{Leading}$ , and  $R_1 \Delta L_{Trailing}$ , respectively. FS: Foot strike, FO: Foot-off, MST: Midstance. Vertical  
 757 lines indicate gait events with the solid line corresponding to the ipsilateral limb while the  
 758 dashed line indicates the contralateral limb.



759  
760 Figure 6. Median changes in pitch impulse following perturbations compared to those measured  
761 during the pre-perturbation step for control participants (Gray, N = 13) and during paretic (Pink)  
762 and non-paretic (Blue) steps for stroke participants (N=38). Each dot represents one participant.  
763 Black horizontal lines indicate the median across participants. Positive values indicate less  
764 forward pitch impulse. (B) The asterisks (\*) indicate whether the group mean is significantly  
765 different from zero (\*p<0.05, \*\*p<0.001).  
766



767  
768 Figure 7. Changes in median net, leading limb, and trailing limb angular impulse during the first  
769 recovery step compared to those measured during the pre-perturbation step. Changes in net  
770 angular impulse (A), leading limb angular impulse (B), and trailing limb angular impulse (C)  
771 during the first recovery step compared to the pre-perturbation step. Each dot represents one  
772 participant. Black horizontal lines indicate the median across participants. The asterisks (\*)  
773 indicate whether values were statistically different from zero (\* $p < 0.05$ , \*\* $p < 0.001$ ,  
774 \*\*\* $p < 0.0001$ ). The hashes (#) indicate when comparisons between groups are significantly  
775 different. Note that for people post-stroke, if the non-paretic leg was perturbed, the leading and  
776 trailing limbs corresponded to the paretic and non-paretic limbs during the first recovery step and  
777 vice versa for the paretic perturbations.  
778  
779



780  
781  
782  
783  
784  
785  
786

Figure 8: Associations between deviation in trailing angular impulse during the first recovery step from the pre-perturbation step in the sagittal plane and clinical assessments. Deviation of trailing angular impulse during the first recovery step from the pre-perturbation step was positively associated with (A) Fugl-Meyer score and (B) the Functional Gait Assessment only following paretic perturbations. FM: Fugl-Meyer; FGA: Functional Gait Assessment.